

# Groundwater salinization in arid coastal wetlands: a study case from Playa Fracasso, Patagonia, Argentina

María del Pilar Alvarez · Cristina Dapeña ·  
Pablo J. Bouza · Ileana Ríos · Mario A. Hernández

Received: 14 April 2014 / Accepted: 9 December 2014  
© Springer-Verlag Berlin Heidelberg 2014

**Abstract** The origin of the high salinity in the groundwater of a coastal wetland in an arid climate was studied in the Playa Fracasso marsh, located on the northwest coast of the extra-Andean Patagonia. Research was carried out by means of the design of a network of soil pits and short piezometers in the marsh and the surrounding landforms. Continuous fluctuations of the water table, in situ physical and chemical properties, major ions ( $\text{Ca}^{2+}$ ,  $\text{Mg}^{2+}$ ,  $\text{Na}^+$ ,  $\text{K}^+$ ,  $\text{Cl}^-$ ,  $\text{SO}_4^{2-}$ ,  $\text{HCO}_3^-$ ) and stable isotopes ( $^{18}\text{O}$  and  $^2\text{H}$ ) in groundwater, as well as soil salinity, were measured. The combined analysis of the hydrodynamics, the ion ratios  $r\text{Ca}^{2+}/r\text{Cl}^-$  and  $r\text{Mg}^{2+}/r\text{Ca}^{2+}$  vs.  $r\text{Cl}^-$  and the isotopic composition made it possible to recognize an area within the high marsh in which the origin of groundwater is mainly marine and another in which the contributions are of mixed origin. By means of the analysis of  $r\text{Cl}^-$  vs.  $\delta^{18}\text{O}$ , a salinization process with no change in isotopic composition was identified. Its interpretation, together with those of the soil salinity profiles and the records of the fluctuations in electrical conductivity associated with extraordinary tides, was used to define a conceptual model of salinization which could be useful to understand other

coastal wetlands under similar arid climatic conditions. It consists in a cyclical mechanism of evapotranspiration, precipitation, dissolution and transport of salts during tides.

**Keywords** Geohydrology · Hydrochemistry · Salt marsh · Patagonia · Arid climate

## Introduction

‘Salt marsh’ is an ecological/morphological term used to refer to low, swampy lands located in the maritime–terrestrial transition and periodically flooded by seawater (Codignotto 1987). They develop under stable geomorphological conditions, such as estuaries or coastal areas protected by spits or barriers, and they are usually covered by halophytic vegetation, tolerant to partial immersion, anoxia and edaphic hypersalinization. The importance of these environments and their study is recognized worldwide due to their enormous primary productivity and the fact that they provide shelter and feeding areas to several invertebrate and vertebrate species of great economic and social relevance (Adam 1990). Besides, the study of the origin of groundwater and its salinity acquires special relevance when assessing the movement of nutrients and the environmental conditions within a marsh, which is a fundamental aspect in its ecohydrological analysis (Mitsch and Gosselink 2000).

The patterns and variations in groundwater flow in a marsh are controlled by the tidal fluctuations, the local water balance (evapotranspiration–precipitation), groundwater discharge from the continent, the geometry and the hydraulic properties of the sediments that constitute it (Wilson and Morris 2012), as well as by its geomorphology (Carol et al. 2013). Tides cause frequent, predictable

---

M. d. P. Alvarez (✉) · M. A. Hernández  
Cátedra de Hidrogeología, Universidad Nacional de La Plata  
(UNLP), CONICET, La Plata, Argentina  
e-mail: alvarez.maria@conicet.gov.ar

C. Dapeña  
Instituto de Geocronología y Geología Isotópica  
(INGEIS, CONICET-UBA), Buenos Aires, Argentina  
e-mail: dapenna@ingeis.uba.ar

P. J. Bouza · I. Ríos  
Centro Nacional Patagónico (CENPAT-CONICET),  
Puerto Madryn, Argentina  
e-mail: bouza@cenpat.edu.ar

hydroperiods affecting the lower parts, whereas in the more elevated ones only extraordinary tides are responsible for the inundation patterns, with the hydroperiods originated by precipitations also being of great relevance (Brinson 1989).

The greater or lesser influence of the continental water supply could be dominant in certain areas (Custodio 2010), which determines whether it is a fresh marsh or a salt marsh (Manzano et al. 2002; Durán 2003; Carol et al. 2009). However, in the most elevated areas, the water patterns are also determined by high salinity, which may be caused by the higher evaporation rate (Silvestri and Marani 2004). Likewise, in arid regions, high salinity characterizes most of the groundwater, with many processes contributing to salinization, among which the mixing with seawater, rainfall concentration, evaporation, evapotranspiration, dissolution of salts and seawater concentration in coastal lagoons are the most common and can lead to groundwater salinities in excess of modern seawater (Ridd and Stieglitz 2002; Fass et al. 2007; Warner et al. 2013).

In the marshes of the arid regions in Patagonia, mainly ecological and edaphological research has been carried out (Bortolus et al. 2009; Bala et al. 2008; Bouza et al. 2008; Ríos 2010; Ríos et al. 2012); and, even if studies on general hydrogeological aspects have been conducted recently (Alvarez et al. 2012), the origin of the high salinity in its groundwater is still the subject of research.

To define a conceptual model of salinization for coastal wetlands in an arid climate, the Playa Fracasso marsh—which has been declared a Ramsar and WHSRN (Western Hemisphere Shorebird Reserve Network) site—was chosen as case study (Fig. 1). By means of the hydrochemical, isotopic and hydrodynamic variables, the influence of marine and continental water and the salinization processes at work were determined.

## Study area

The study area, located on the coast of the San José Gulf within the Área Natural Protegida Península Valdés (Península Valdés Protected Natural Area), corresponds to an open coast and bay marsh (Bouza et al. 2008) with no inflow from permanent surface watercourses. It is located in the discharge area of the regional aquifer system (Alvarez et al. 2010), a phenomenon that is evident in the spring occurring on the cliffs limiting the area to the NE (Fig. 1).

The mean annual precipitation is 230 mm, with no definite trend throughout the year, and a mean annual temperature of 13.4 °C, fluctuating between mean extremes of 6.4 °C in July and 20.4 °C in January. The potential evapotranspiration, estimated for reference

following Thornthwaite and Mather (1957), is 700 mm/year. As regards the relative humidity, the mean annual value is 68.4 % and the monthly mean varies between 62.4 % in January and 75.5 % in June. Such behaviour is expected for the extra-Andean Patagonian region, where the relative humidity values are low and their concentration in winter is aided by the low temperatures as well as by the lower frequency and intensity of the winds.

Under such conditions, the climate is classified as arid, mesothermal according to Thornthwaite (Burgos and Vidal 1951). To carry out the climate characterization, the records of the weather station of the Centro Nacional Patagónico (CENPAT; National Patagonian Centre) between 1982 and 2002 (Frumento and Contrera 2013) were used, together with the precipitation data ranging from 1901 to 2006 of the Estancia La Adela (La Adela Farm); these are located approximately 95 km to the SW and 20 km to the SE of Playa Fracasso, respectively.

The material outcropping in cliffs and in the erosion scarps surrounding the marsh is mainly represented by tertiary sediments of marine origin of the Puerto Madryn formation (sand, silt and clay with an important tuffaceous component and intercalations of shell and gypsum levels), Plio-Pleistocene gravel of the Rodados Patagónicos (Patagonian Shingle Formation) and quaternary alluvial and colluvial deposits, which are a remobilization of the above-mentioned deposits (Haller et al. 2001). On the coast, there are thin eolian layers (no more than 0.5 m), which mainly overlie the alluvial deposits.

From a geomorphological point of view, Playa Fracasso is a vast tidal plain which is overlain by a marsh (M) of approximately 35 ha (0.35 km<sup>2</sup>), crossed by tidal channels and associated with spits (E1 and E2), *bajadas* (B1 and B2), sandy layers (SL) and pediments (Pd and PdF) (Fig. 1).

The origin of the marsh is related to sea level fluctuations and the littoral drift—both of which generate sand bars that lie along the coastline—as well as to the accretion of a spit following a west–east trend (Ríos 2010). Topographically, it is a low area, with heights that do not exceed 8 m asl and a gentle slope, where drainage is generally deficient. The marsh shows a vegetation zonation characterized by *Spartina alterniflora* in the lower part, and *Sarcocornia perennis* and *Spartina densiflora* in the upper part. In the tidal-channel levees, which constitute relatively high areas, patches of *Limonium brasiliense* can be observed.

The soils associated with the marsh were classified by Ríos et al. (2012), according to the USDA Soil Taxonomy (Soil Survey Staff 1999), as Sodic Endoaquents and Sodic Psammaquents in the area dominated by *S. alterniflora*, Typic Fluvaquents in the area with *S. perennis* and in the patches with *L. brasiliense*.

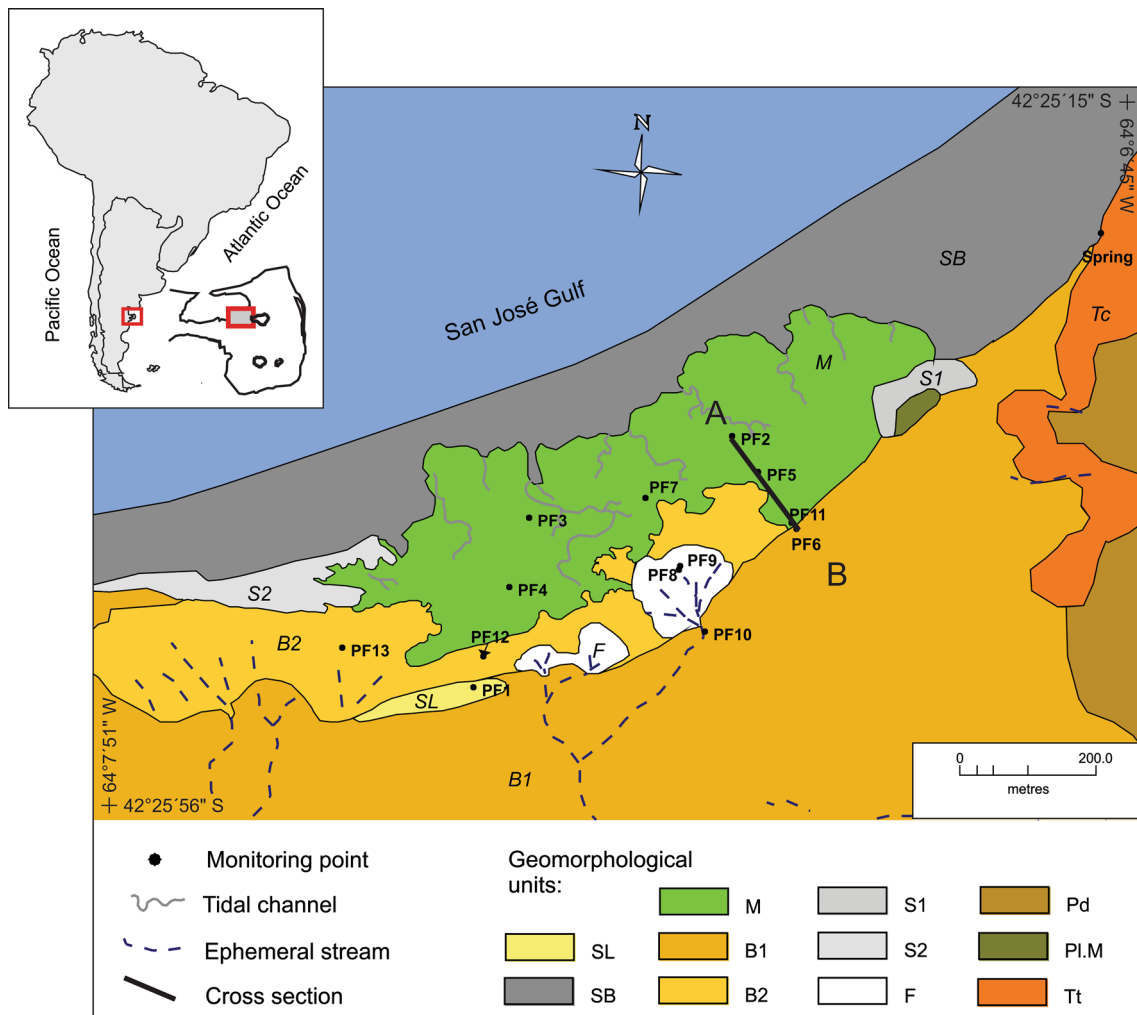


**Fig. 1** Location map and geomorphological units. Geological designations are as follows: *SL* sandy layer, *SB* sandy beach, *M* marsh, *F* alluvial fan, *B1* and *B2* coalescent alluvial-fan piedmont or *bajada*,

*S1* and *S2* spit, *Pd* pediment, *Pl. M* palaeommarsh, *Tt* tertiary sediment erosion scarp, *AB* cross section [modified from Alvarez et al. (Alvarez et al. 2012)]

The marsh is crossed in its middle and lower sections by active tidal channels (Fig. 1). Depending on the tidal range, the water flowing into these channels affects the marsh to a greater or lesser extent, flooding it almost entirely during extraordinary high tides, in which the range exceeds 8 m according to the records of the Argentine Navy Hydrographic Service (Hidrografía Naval Argentina 2010–2012), whereas during ordinary high tides seawater is either circumscribed to the channel or it overflows, only reaching the lowest lying areas.

**Materials and methods**

A monitoring network consisting of 13 shallow manually drilled boreholes (depths up to 2.3 m) was set up to carry out this research. The spatial distribution of these

piezometers was based on geomorphological information obtained in the field and by satellite image interpretation. They mainly correspond to three transects perpendicular to the coastline, extending from the littoral *bajadas* to the high marsh (Fig. 1). The boreholes were levelled with an optical level (Kern GK1-AC) and, adjacent to each one, a pit was dug to describe the soil profile, including soil texture, and to obtain samples of the soil horizons to measure their electrical conductivity (EC).

About 40 water samples [i.e. groundwater (PF), spring water and seawater] were collected in three sampling fieldworks (i.e. November 2010, August 2011 and February 2012), and analyzed for their chemical and isotopic compositions. The pH, temperature and EC, as well as the piezometric levels, were measured in the field, always during the low tide period.

To analyze the influence of the tides, by monitoring the water-table fluctuations and salinity variations, three automatic water-level dataloggers (two Schlumberger Cera-Divers and one Schlumberger CTD-Diver) were installed in piezometers PF5, PF6 and PF11. All of them were set to record data at 15-minute intervals. The salinity monitoring datalogger (EC) was located at point PF11.

Chemical analyses of major elements were carried out by the Chemical Service of the CENPAT laboratory. The  $\text{Ca}^{2+}$ ,  $\text{Mg}^{2+}$ ,  $\text{Na}^+$ ,  $\text{K}^+$ ,  $\text{Cl}^-$ ,  $\text{SO}_4^{2-}$ ,  $\text{HCO}_3^-$  and  $\text{NO}_3^-$  determinations were performed by the conventional methods in accordance with the American Public Health Association (APHA, AWWA and WPCF 1997). Ion ratios ( $r$ ) were calculated with the Easy Quim (Vázquez Suñé 2002) and AquaChem (Schlumberger 2010) applications.

The water isotopic analyses were carried out by the Instituto de Geocronología y Geología Isotópica (INGEIS, Geochronology and Isotope Geology Institute) of the Consejo Nacional de Investigaciones Científicas y Técnicas (CONICET, National Scientific and Technical Research Council) and the Universidad de Buenos Aires (UBA, University of Buenos Aires), Argentina. Samples were treated following conventional techniques and measured using Los Gatos Research high-precision laser spectroscopy, i.e. off-axis integrated cavity output spectroscopy (Lis et al. 2008). Results are expressed using the conventional  $\delta$ -notation, defined in Eq. (1).

$$\delta = 1000(R_s - R_p)/R_p \text{ [‰]}, \quad (1)$$

where  $\delta$  is the isotope deviation in ‰,  $s$  the sample,  $p$  the international reference, and  $R$  the isotope ratios ( $^2\text{H}/^1\text{H}$ ,  $^{18}\text{O}/^{16}\text{O}$ ). Values are relative to the Vienna Standard Mean Ocean Water (VSMOW) (Gonfiantini 1978). Uncertainties are  $\pm 0.3$  ‰ for  $\delta^{18}\text{O}$  and  $\pm 1.0$  ‰ for  $\delta^2\text{H}$ .

The isotopic composition of rainwater was compared with data from the rain collection station at Puerto Madryn, Chubut province, for the periods October 1981–April 1985 and December 1998–November 2006, and with the local meteoric water line as defined by Dapeña (2008) with 43 records, i.e.  $\delta^2\text{H} \text{ ‰} = (7.37 \pm 0.22) \cdot \delta^{18}\text{O} - (0.36 \pm 1.70) \text{ ‰}$  for this station. The rain collector is part of the Red Nacional de Colectores (National Collection Network) setup by the INGEIS within the framework of the Global Network for Isotopes in Precipitation (GNIP), created by the International Atomic Energy Agency and the World Meteorological Organization (IAEA/WMO 2002; Dapeña and Panarello 1999, 2008). These measurements were supplemented by meteorological information, such as the mean surface air temperature and the amount of precipitation. The record is incomplete due to lack of precipitation or insufficient amounts of rain; besides, there were periods in which no samples could be obtained. However, a preliminary meteoric line and some weighted averages for the

years 1999, 2000, 2005 and 2006 were calculated. The arithmetic mean is  $\delta^{18}\text{O} = -7.2$  ‰ and  $\delta^2\text{H} = -52$  ‰,  $d = 6$  ‰ with 43 records. The isotopic composition of the precipitation shows great dispersion, with values ranging from  $-12.9$  to  $-0.9$  ‰, and from  $-86$  to  $-4$  ‰ for  $\delta^{18}\text{O}$  and  $\delta^2\text{H}$ , respectively.

The data were represented in a conventional  $\delta^2\text{H}$  vs.  $\delta^{18}\text{O}$  diagram with the local meteoric water line. Also a chloride vs.  $\delta^{18}\text{O}$  graph was plotted to evaluate the salinization mechanisms.

## Results

The salinization processes in the marsh were analyzed considering the hydrodynamics and the salt content in the soil profile, together with the hydrochemistry and the isotopic composition of water.

### Hydrodynamics

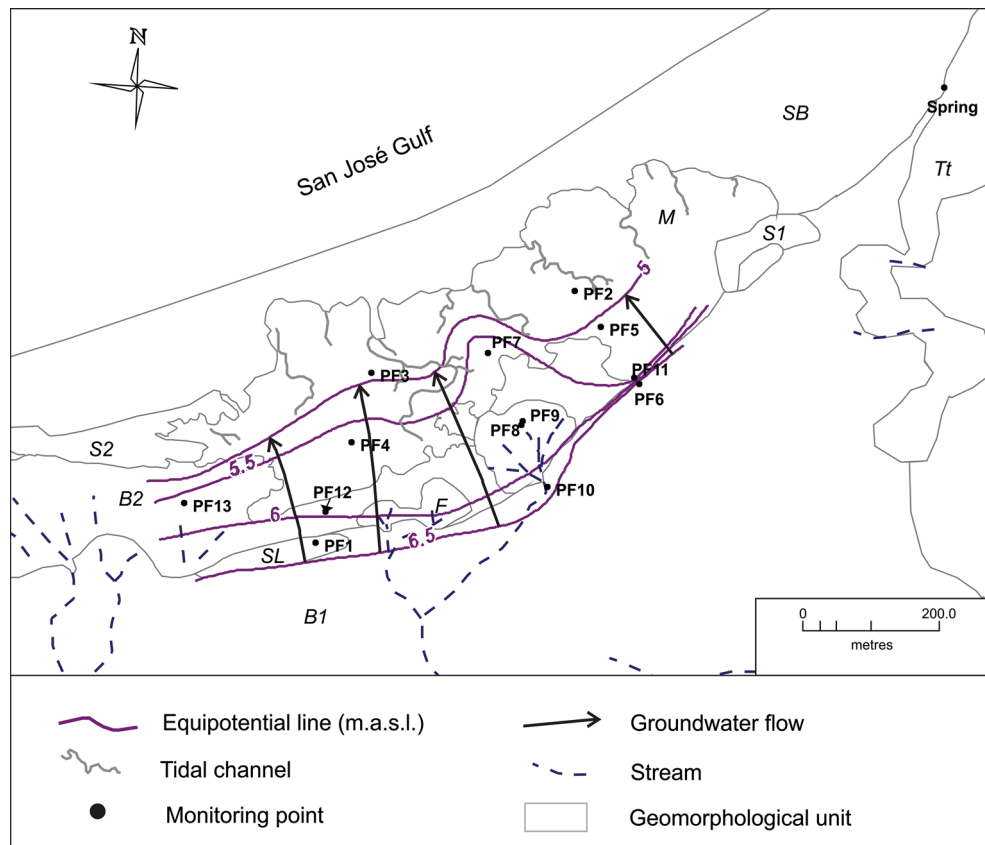
As regards the surface inflow of continental origin—peninsular, in this case—it is exclusively ephemeral, in a SE–NW direction and it corresponds to the discharge, during storm events, of the littoral *bajadas*, as shown by the alluvial landforms that surround and overlie part of the marsh (Fig. 1).

Concerning the hydrodynamic behaviour, three sectors were identified: (1) of preferential recharge, represented by units B1, B2 and SL; (2) of circulation, directly associated with the marsh; and (3) of discharge along the coastline. The groundwater flow defined has a general SSE–NNW direction, perpendicular to the coastline and to the limit between the marsh and the *bajadas* (Fig. 2).

The fluctuations of the water table, recorded by means of the different divers installed along the AB transect (Fig. 1), are shown in Fig. 3. In the one closest to the coast (PF5), a cyclical repetition of sets of maximum fluctuations can be observed approximately every 28 days (150 cm between the minimum and maximum values), as well as some minor ones intercalated every 14 days. In the diver installed in an intermediate location (PF11), the oscillation follows a similar pattern, with maximum peaks coinciding in time with the ones recurring every 28 days in PF5, although the range never exceeds 130 cm. In the case of PF6, only some peaks coinciding with those of PF5 and PF11 are reproduced, and its range barely reaches 48 cm.

Even though there is no tide gauge locally available which would make it possible to compare the water table levels with those of the tides accurately, the predictions of the Servicio de Hidrografía Naval Argentino for Playa Fracasso (Hidrografía Naval Argentina, 2010–2012) indicate that spring tides, whose recurrence is approximately

**Fig. 2** Equipotential map for November 2010. Geomorphological unit references are as shown in Fig. 1. Modified from Alvarez et al. (2012)



every 14 days, have a range between low and high tide oscillating between 7 and 9 m and that these coincide in time with the maximum water table fluctuations observed in the records of the divers installed in PF5, PF11 and PF6.

In aquifer sediments hydraulically connected to the sea, the level fluctuations occurring in the water body are transmitted landward as continuous variations in the groundwater levels (Ferris 1951; Erskine 1991; Smith and Hick 2001; Bye and Narayan 2009). The cyclical rises in the water table recorded by divers PF5 and PF11 show the influence of the tidal fluctuations, with maximum peaks with a recurrence similar to the one of the spring tides. The combined analysis of these records and the isophreatic map (Fig. 2) indicates inundation events in the marsh up to its upper end, in the limit with the *bajadas* (Fig. 1).

By way of summary, in Fig. 4 a schematic cross section of the hydrodynamic behaviour of the marsh and the relationship between marine and continental groundwater inflow are shown. This transect coincides with wells PF2, PF5, PF11 and PF6 (Fig. 1).

#### Soil salinity profile

Together with the groundwater sampling and the level and EC records of the divers, the EC of the soil was

measured in soil pits coinciding with wells PF5, PF11 and PF6 (Fig. 5). The soil profiles located in the marsh (PF5 and PF11) are composed of an A horizon with a silty to silty loam texture overlying sandy C horizons. Soil pit PF5 shows a salinity profile with EC values ranging between 13 and 13.8 mS/cm on the surface, and it decreases gradually with depth up to a value of 9.14 mS/cm. In profile PF11, a high salinity value (EC 44.10 mS/cm) can be observed, being localized in the first horizon and decreasing abruptly below the upper 20 cm, reaching lower values than those recorded in PF5. It is important to highlight that in both edaphic profiles the sediments are of marine origin and that they belong to similar textural classes; however, the significant difference in soil salinity in the upper centimetres indicates that it is not the parent material that is responsible for such a variation, but the presence of a salinization mechanism. In turn, in the profile located over the *bajada* landform (PF6) of the type A–AC–C, a sandy texture with intercalations of shell remains and gravels predominates and the conductivity in the different levels is much lower than in the marsh soils. Up to a depth of 113 cm, the EC values remain below 0.2 mS/cm and, as from that point up to a depth of 140 cm — coinciding at the time of describing the profile with the



water table (saturated zone) and with the presence of buried beach sand—they increase until they reach values of 2.2 mS/cm (Fig. 5).

### Hydrochemistry

#### Saline content

The water salt content varies spatially between 4.6 and 88.2 g/L depending on its location (i.e. marsh, fans, *bajadas*, sandy layer, spring or sea), with an increasing gradient towards the centre of the area, and temporally depending on the season and the tides.

The temporal EC fluctuations recorded at PF11 show that the most significant variations occur with a certain cyclicity and are associated with the highest water fluctuation levels. The highest EC records are associated with the instance in which the water level is above ground level, a situation that occurs cyclically and is related to the spring tides. Besides, as the highest temperatures are approached (November–January), the records increase in value. In August, the contents do not exceed 40 mS/cm, whereas in December they are higher than the measurement limit of the instrument (80 mS/cm). As regards the behaviour in between spring tides, it can be observed that when the water table decreases, so does the EC, remaining in the winter months between 20 and 30 mS/cm and in the summer months above the marine value (Fig. 3).

It should be clarified that the periods in which the records are null (EC = 0 mS/cm) correspond to measurements in which the diver was out of the water due to a further decrease in the water table. Such decreases occur between November and January, when evapotranspiration is highest and the general level of the whole marsh is deeper.

#### Ionic composition

According to the Piper classification, in the sampled groundwater associated with the marsh, the littoral *bajadas* and the spring, the predominant ions are Na<sup>+</sup> and Cl<sup>-</sup>. Sodium increases linearly with respect to chloride, showing a high correlation index (Fig. 6a), with the

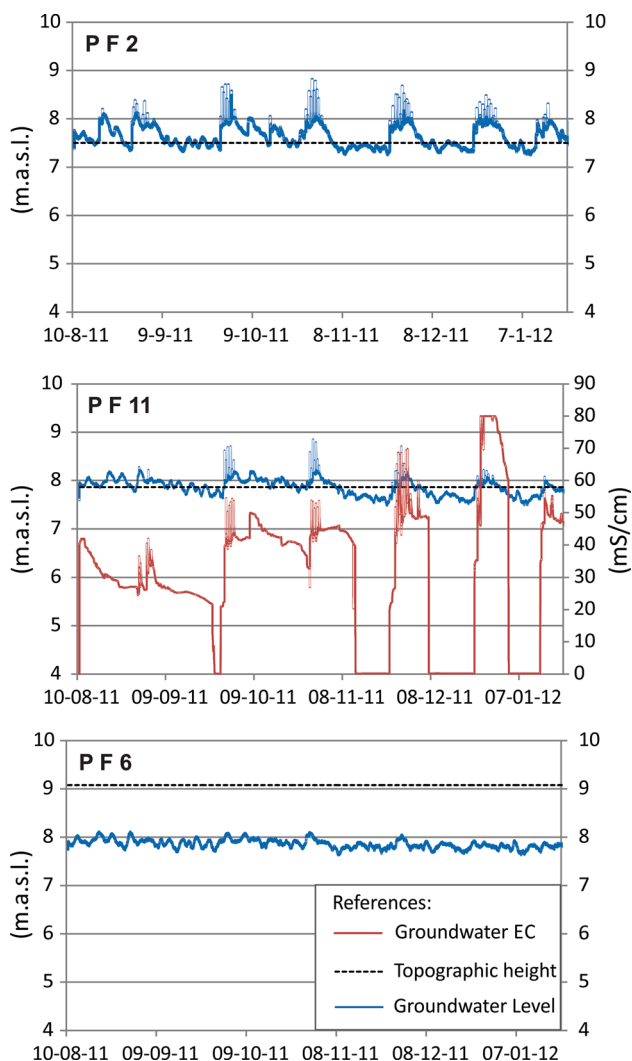


**Fig. 3** Groundwater level and electrical conductivity fluctuations registered by divers located at points PF5, PF11 and PF6

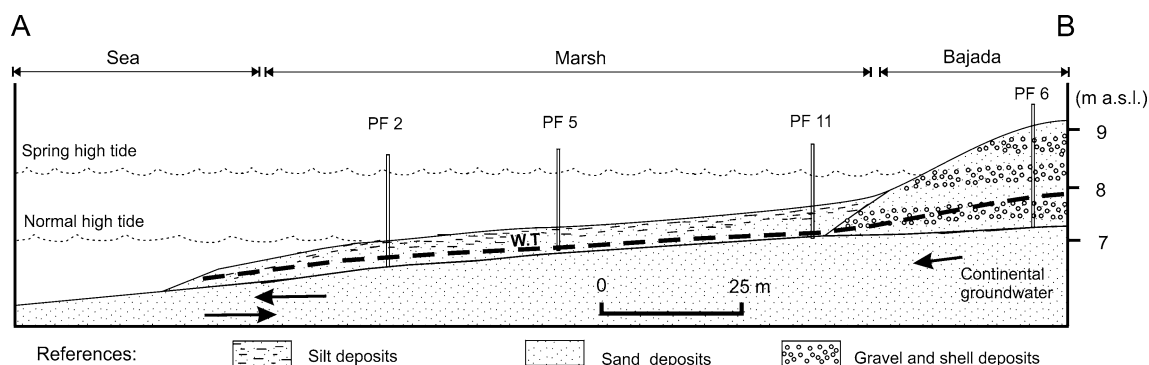


**Fig. 4** Schematic cross section of the hydrodynamic behaviour of the saltmarsh

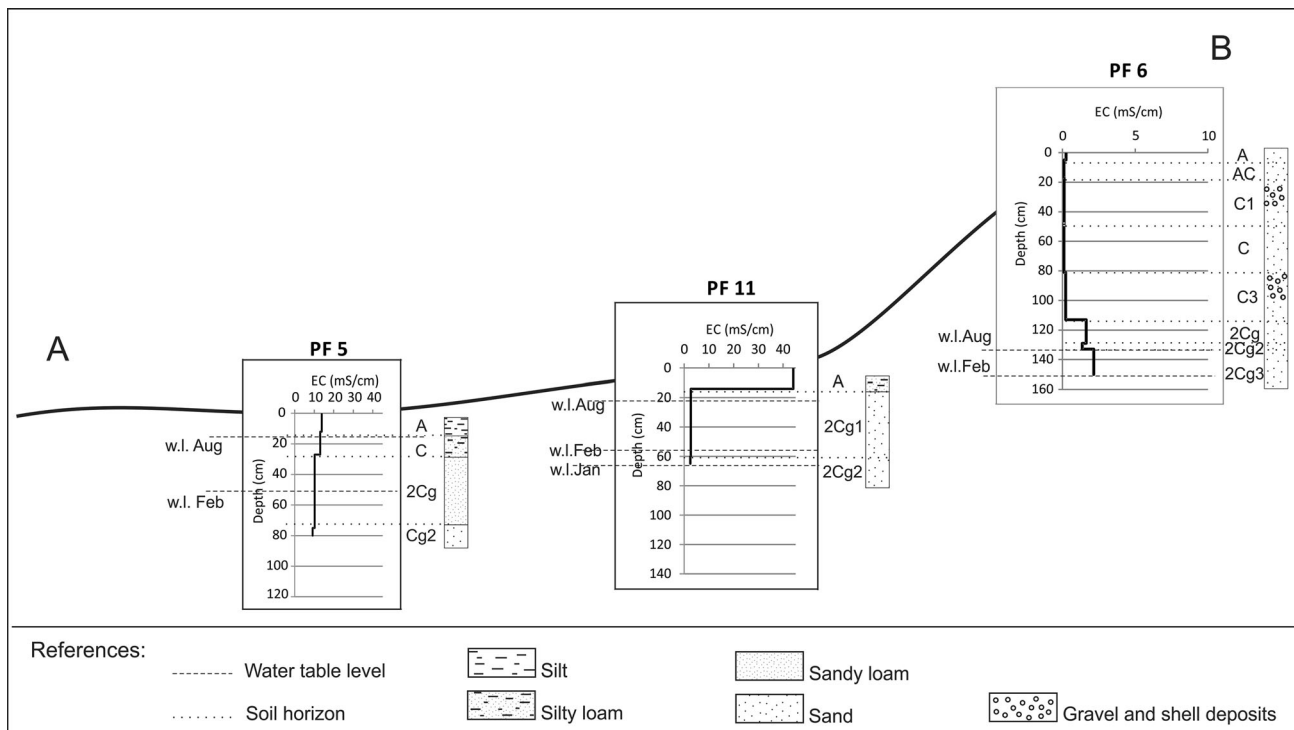


**Fig. 5** Schematic location of the soil profiles in the AB cross section. Capital letters are used to designate master horizons; arabic numerals are used both as suffixes to indicate vertical subdivisions within a

horizon and as prefixes to indicate discontinuities; suffix *g*: strong gleying in which iron has been preserved in a reduced state because of saturation with stagnant water

samples corresponding to the *bajadas* and the spring being the least saline and the ones of the fans, the most saline. In an intermediate position between such extremes are the sea samples, whereas the marsh samples are distributed practically along the entire correlation line with a ratio close to 0.84, which is within the range of the marine values measured (0.83, 0.81 and 0.9). Among these, the PF11 samples fluctuate between lower values ( $Cl^-$  238 meq/L) and similar or higher values ( $Cl^-$  551.5 meq/L) than the ones of the sea ( $Cl^-$  545.5 meq/L). The PF2 values are similar to the ones of the sea,

except in the sample obtained in February ( $Cl^-$  633.8 meq/L) (Fig. 6a).

In general, the increase in  $Na^+$  and  $Cl^-$  content indicates seawater intrusion (Lee and Song 2007), even though it may be related to evaporitic levels or fossil marine water (Castillo Pérez and Morell Evangelista 1988). Besides, the halite content in marine aerosols may cause rain events with a water composition of the sodium chloride type. In addition, the groundwater discharge of continental origin is  $Cl^-Na$ ; therefore, the contrast between the marine and continental contributions is not evident.

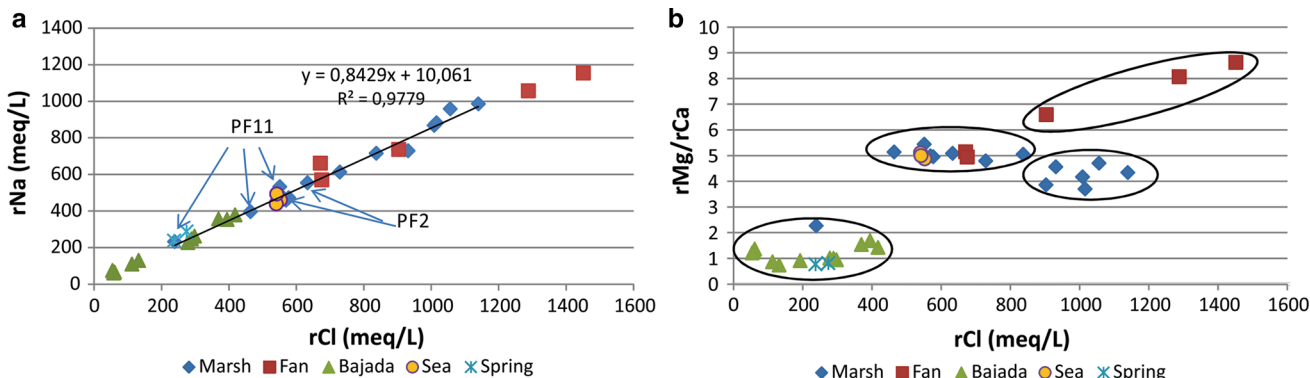


**Fig. 6** Scatter plot of selected parameters from groundwater, spring and seawater samples, expressed in meq/L, and their ratios: rNa vs. r Cl (a), and rMg/rCa vs. rCl (b)

The  $r\text{Mg}^{2+}/r\text{Ca}^{2+}$  ratio increases as the proportion of seawater in a mixture is higher, as in seawater there is an excess of  $\text{Mg}^{2+}$  with respect to  $\text{Ca}^{2+}$  (Custodio 1997). In Fig. 6b, the samples are organized into four groups. One of them with  $r\text{Mg}^{2+}/r\text{Ca}^{2+}$  ratios near 1, among which the spring sample can be found, as well as all of the samples associated with the *bajadas* and one of the marshes (PF11), in which the continental groundwater flow would predominate. Another group is composed of seawater ( $r\text{Mg}^{2+}/r\text{Ca}^{2+} \sim 5$ ) and other samples with similar values (practically all of the marsh samples, as well as two of the fan samples) whose origin is related to the marine contribution. The third group consists of marsh samples associated with wells PF4 and PF7, whose ratio lies between the marine and continental values (3.69–4.55), suggesting a mixed origin. Finally, there is a group of three samples associated with the alluvial fans in which the ratio is much higher than 5, and in turn have a high chloride content (PF8 and PF9). In this last group, given its high salinity and its spatial location, it is probable that other modifying processes, such as base exchange or  $\text{Ca}^{2+}$  precipitation, could be distorting the interpretation of this ratio (Custodio 1997; Appelo and Postma 2005).

## Isotopes

### $\delta^2\text{H}$ vs. $\delta^{18}\text{O}$

The isotopic compositions of all the samples (marsh, *bajadas*, sandy layer, fans, spring and sea) are represented in the conventional  $\delta^2\text{H}$  vs.  $\delta^{18}\text{O}$  plot (Fig. 7).

The isotope content of the groundwater samples of the *bajadas* (PF6, PF10, PF12 and PF13) and of the sandy layers (PF1) has  $\delta^{18}\text{O}$  values between  $-7.0$  and  $-4.6$  ‰ and  $\delta^2\text{H}$  values between  $-61$  and  $-43$  ‰, which reflects the values of local precipitation. However, PF12 and PF13 have a more enriched composition, indicating evaporation processes (Fig. 7). The fans (PF8 and PF9) have  $\delta^{18}\text{O}$  and  $\delta^2\text{H}$  contents between  $-4.5$  and  $-2.5$  ‰ and between  $-43$  and  $-33$  ‰, respectively. Together, the *bajadas* and fans are aligned along an evaporation line, i.e.  $\delta^2\text{H} = 5.3\delta^{18}\text{O} - 19.9$  (Fig. 8). Nevertheless, the fans have very high-salt values which cannot be justified by the evaporation alone, and which are probably related to the action of several processes taking place simultaneously, like transpiration, base exchange and salt dissolution.

The spring samples have a  $\delta^{18}\text{O}$  composition between  $-5.4$  and  $-2.3$  ‰ and a  $\delta^2\text{H}$  composition between  $-56$  and  $-38$  ‰, indicating variations in the isotope content of the regional groundwater flow discharge (Fig. 7).

The marsh groundwater (PF2, PF4, PF5, PF7 and PF11) has  $\delta^{18}\text{O}$  values between  $-5.2$  and  $0.4$  ‰ and  $\delta^2\text{H}$  values between  $-42$  and  $1$  ‰. Even though most values are

located near the position of the local seawater ( $\delta^{18}\text{O}$  between  $-0.3$  and  $0.1$  ‰;  $\delta^2\text{H}$  between  $-3$  and  $-1$  ‰), they show a chloride content which is twice as high as the one in seawater. However, PF4 and PF11 are relatively more depleted, and PF11 in particular has very high salinities but with a high variability among sampling periods, also showing mixtures between waters such as the ones in PF6 (*bajada*) and in PF4 (marsh). These mixes are variable and close to 26 and 47 % in November and August, respectively.

## Discussion

The hydrodynamic and hydrochemical analyses ( $r\text{Mg}/r\text{Ca}$  ratio) show a mixed origin for the marsh groundwater, but cannot explain the hypersaline composition of some waters, which indicates the existence of other salinization processes. Although the  $r\text{Na}/r\text{Cl}$  ratio close to the marine value suggests that the evaporation of seawater below the halite saturation state could be one of the salinization processes, the hypersaline waters do not have an isotopic signature consistent with marine water evaporation. Neither does it appear to be derived from geological or anthropogenic sources, considering that the lithology of the soil profiles analyzed at the cross section is the same for both marsh points and that it is an unpopulated area. On the basis of these data, it can be interpreted that the isotopic compositions and salinities of the samples do not respond exclusively to the marine contribution, but rather to the joint action of several processes, such as evapotranspiration, mixing, marine aerosols and dissolution/precipitation (Gat 1981; Harbison and Cox 2002; Vengosh 2003; Fass et al. 2007).

The conservative elements  $\text{Cl}^-$  and  $^{18}\text{O}$  were analyzed, as they have traditionally been used to study the salinization processes (Gonfiantini and Araguas-Araguas 1988; Yurtsever 1994; de Montety et al. 2008; Han et al. 2011). In Fig. 8, which shows the scatter plot of  $r\text{Cl}^-$  vs.  $\delta^{18}\text{O}$ , it can be observed that the samples located in the marsh (PF2, PF4, PF5 and PF7) have a relatively constant isotopic composition among samplings, which, on the whole, is similar to the one of the sea. Their salinities, however, exceed the values of the marine samples in all cases.

The behaviour of these points, in which there are no changes in isotopic composition and whose  $\text{Cl}^-$  content is higher than the value of the sea, can be explained as a cyclical mechanism of evapotranspiration, subsequent salt precipitation, new seawater inflow and the consequent partial dissolution of the precipitated salts (Fig. 8). In addition, another process that contributes to the high salinity and to the lack of changes in the isotopic



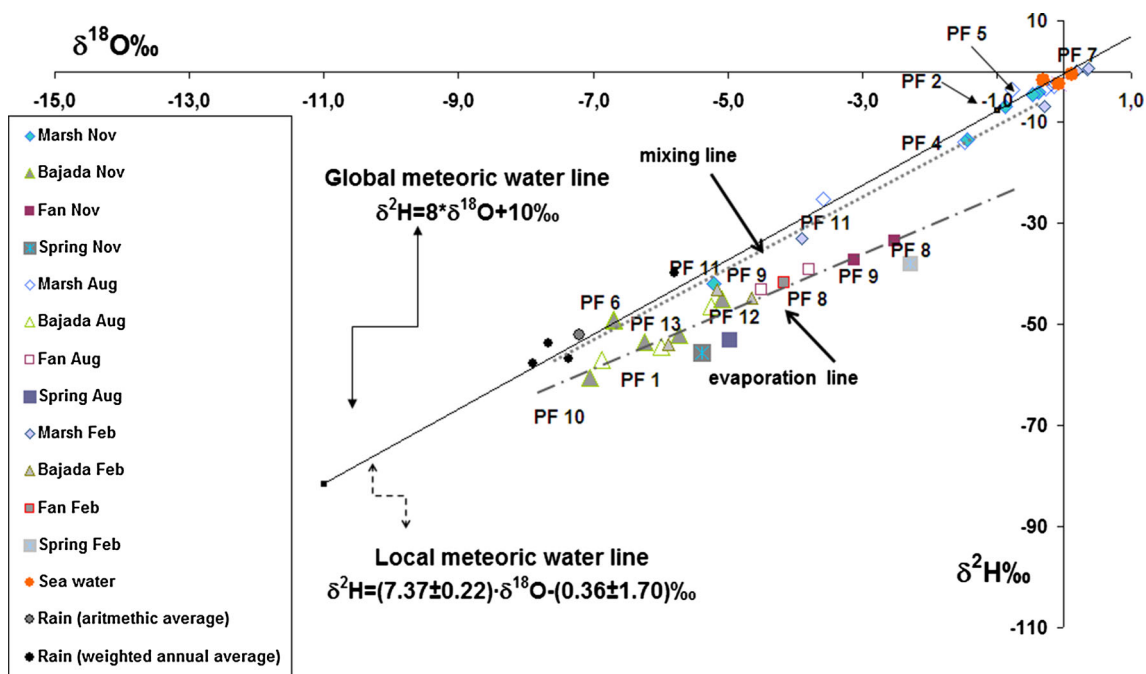
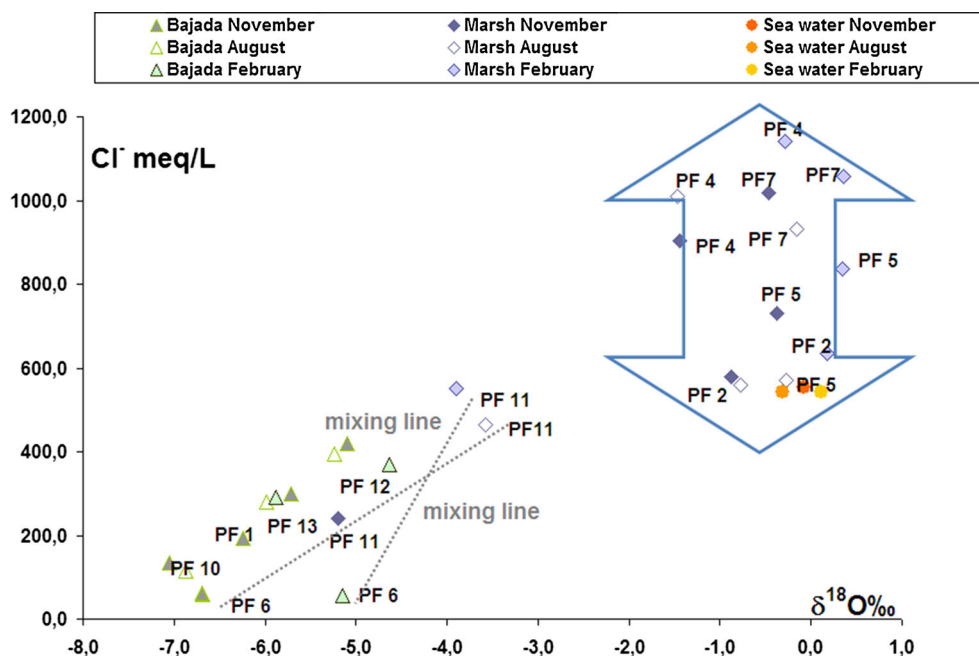


Fig. 7  $\delta^2\text{H}$  vs.  $\delta^{18}\text{O}$  plot for all groundwater samples, spring, San José Gulf Sea and the local meteoric water line

Fig. 8  $\text{rCl}^-$  vs.  $\delta^{18}\text{O}$  plot for the marsh and *bajada* groundwater samples and the San José Gulf Sea. The arrow shows marsh samples with no significant change in isotope composition but significant variations in chloride concentration



composition could be plant transpiration. For example, according to Fass et al. (2007), highly saline groundwater occurs beneath mangrove vegetation without inducing isotopic fractionation, and this is attributed to the exclusion of salts during the transpiration of tidal seawater.

On the other hand, the isotopic composition, as well as the ion content measured in well PF11 during the

three samplings, reflects a mixing process between the groundwater of the marsh and of the *bajadas* (Figs. 7, 8). However, the continuous records of salinity fluctuations (Fig. 3) and the high salinity in the upper centimetres of the soil profile (Fig. 5) suggest that the cyclical mechanism described in the previous paragraph also occurs.

Proposed conceptual model

The chemical evolution of solutes in arid continental environments has been explained by Fitzpatrick et al. (2000) for Australia by means of a salinization cycle that involves salt accumulation on the ground, evaporation, total desiccation, precipitation–dissolution of minerals and then the flushing of the accumulated salts into the unsaturated zone.

In the case of the marsh in Playa Fracasso, it is a coastal environment in an arid climate, with tidal influence and a limited brackish continental inflow. Taking into consideration that the high salinity of the upper centimetres of the soil profile corresponds to an evaporation profile and suggests the presence of precipitated salts, together with the coincidence of the highest groundwater salinization peaks with the highest water tables recorded in well PF11 and the hydrodynamic, hydrochemical and isotopic characteristics described, a simplified salinization model is proposed, as shown in Fig. 9.

In this figure, the cycle begins with the increase in groundwater level induced by normal tides (1), followed by the capillary rise and evaporation of saline water and evapotranspiration in the unsaturated zone (2 and 3), which results in the precipitation of salts in the upper portion of the soil (4). Then, at the high spring tides, the salt water that floods the marsh dissolves the salts accumulated on the surface and in the upper centimetres of the soil (5), and transports them at low tide towards the saturated zone, causing the hypersalinization of groundwater (6).

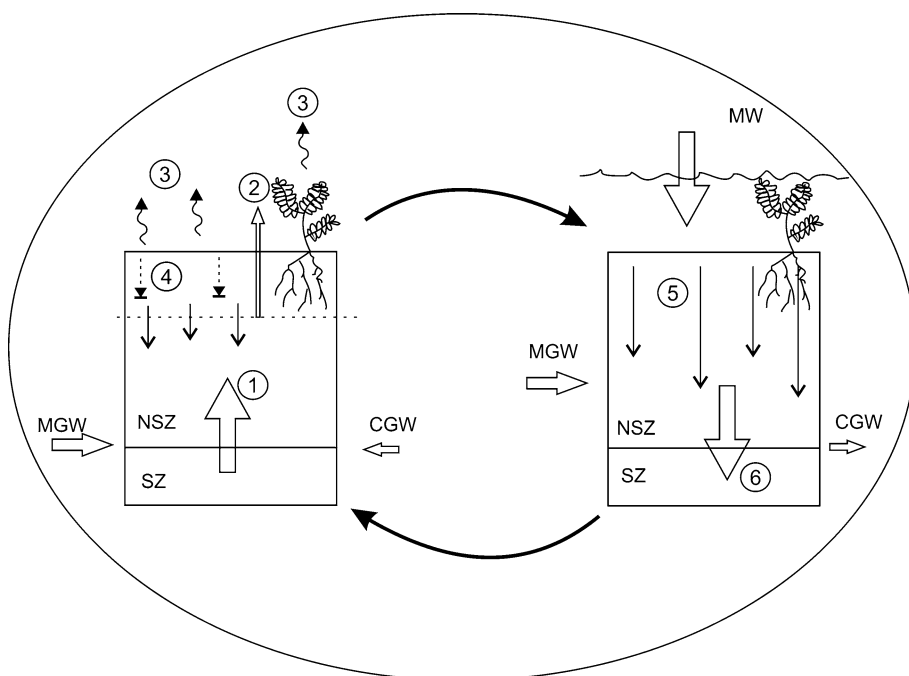
Conclusions

The combined analysis of the hydrodynamics, hydrochemistry and isotopic composition indicates that there is a section within the high marsh in which the source of groundwater is mainly marine, and another in which the contributions are of mixed origin. The groundwater in the marsh, the surrounding landforms, and the spring is sodium chloride type water and it has very high salinity, however, the analysis of the soil profiles indicates that the parent material is not responsible for the high salinity of the system.

Regarding the marine influence over the marsh, the water table fluctuation records measured by the divers show a recurrence every 28 days, indicating the scope—even in the distal section of the marsh—of the extraordinary tides with the widest ranges. But the  $rMg^{2+}/rCa^{2+}$  ratios vs.  $rCl^{-}$  made it possible to differentiate an area with continental contribution, represented by the *bajadas*, the sandy layer and the spring, and another with marine contribution, constituted by the marsh. However, within this area, point PF11 shows a mixed origin. The analysis of  $rNa^{+}$  vs.  $rCl^{-}$  was not useful to differentiate marine and continental contributions but it was helpful to understand the salinization processes.

On the basis of the isotopic composition ( $^{18}O$  and  $^2H$ ), it was possible to identify clearly the continental and meteoric origin of the groundwater associated with the landforms of the *bajadas*, fans and the spring, as well as the evapotranspiration processes. When  $Cl^{-}$  was considered, a

**Fig. 9** 1 Saline groundwater rise by normal tide fluctuations; 2 capillary evaporation of rising groundwater; 3 evapotranspiration; 4 soil salinization/salt precipitation; 5 dissolution and 6 transport of soluble salts into the unsaturated zone. MW marine water, MGW marine groundwater, CGW continental groundwater, NSZ non-saturated zone, SZ saturated zone



cyclical mechanism was identified for the marsh samples, involving evapotranspiration, precipitation and dissolution with no changes in the isotopic composition, whereas in the high part of the marsh the mixture with continental water was observed. The origin of the groundwater in the *bajadas* can be associated with local rainwater infiltration and regional discharge.

On the basis of the cyclicity of the salinity fluctuations and the association with extraordinary tides, the soil salinity profiles and the salinization with no changes in the isotopic composition of groundwater, a conceptual model of salinization for the marsh with a cyclical mechanism of evapotranspiration, precipitation and salt dissolution by seawater leaching was defined, which could be useful to understand other coastal wetlands under similar arid climatic conditions.

**Acknowledgments** The authors would like to thank Agr. Eng. Claudia Saín for her assistance in the laboratory and Tech. Julio César Rua (Bocha) for his help in the field. This work has been funded by the ANPCyT (PICT2008 No 2127) and the CIUNPAT-UNPSJB-PROPEVA (PI No 842).

**References**

Adam P (1990) Salt marsh ecology. Cambridge University Press, Cambridge

Alvarez MP, Weiler N, Hernández MA (2010) Linking geomorphology and hydrodynamics: a case study from Peninsula Valdés, Patagonia. *Argent Hydrogeol J* 18:473–486

Alvarez MP, Dapeña C, BouzaP, Hernández MA (2012) Estudio químico e isotópico preliminar del origen del agua subterránea en el humedal costero Playa Fracasso. Peninsula Valdés, Chubut. II Reunión Argentina de Geoquímica de la Superficie. IADO. CONICET-UNS. Bahía Blanca. Abstract book. GI-1

APHA, AWWA, WPCF (1997) Standard methods for the examination of water and waste water, 19th edn. American Public Health Association, Washington, p 1134

Appelo CAJ, Postma D (2005) Geochemistry, groundwater and pollution. CRC Press. Taylor & Francis Group. 241–247

Bala LO, Hernández MA, Musmeci LR (2008) Humedales costeros y aves playeras migratorias. CENPAT, Puerto Madryn, p 120. ISBN:978-987-05-5598-8

Bortolus A, Schwindt E, Bouza PJ, Idaszkin YL (2009) A characterization of Patagonian Salt Marshes. *Wetlands* 29(2):772–780

Bouza PJ, Sain C, Bortolus A, Ríos I, Idaszkin Y, Cortés E (2008) Geomorfología y características morfológicas y fisicoquímicas de suelos hidromórficos de marismas patagónicas. Actas XXI Congreso Argentino de la Ciencia del Suelo, San Luis. CD-ROM edition

Brinson MM (1989) Fringe wetlands in Albemarle and Pamlico sounds: landscape position, fringe swamp structure, and response to rising sea level. Project No. 88-14, Albemarle-Pamlico Estuarine Study, Raleigh

Burgos JJ, Vidal AL (1951) Los climas de la República Argentina, según la nueva clasificación de Thornthwaite. *Meteoros* 1:3–32

Bye JAT, Narayan KA (2009) Groundwater response to the tide in wetlands: observations from the Gillman Marshes, South Australia. *Estuar Coast Shelf Sci* 84:219–226

Carol E, Kruse E, Mas-Pla J (2009) Hydrochemical and isotopical evidence of ground water salinization processes on the coastal plain of Samborombón Bay. *Argent J Hydrol* 365:335–345

Carol E, Mas-Pla J, Kruse E (2013) Interaction between continental and estuarine waters in the wetlands of the northern coastal plain of Samborombón Bay. *Appl Geochem* 34:152–163

Castillo Pérez E, Morell Evangelista I (1988) La hidroquímica en los estudios de intrusión marina en los acuíferos españoles. *TIAC* 88, 19–73

Codignotto JO (1987) Glosario Geomorfológico Marino. Asociación Geológica Argentina, Serie B: Didáctica y Complementaria No. 17, p 70

Custodio E (1997) Studying, monitoring and controlling seawater intrusion in coastal aquifers. In: guidelines for study monitoring and control. FAO Water Reports, p 11

Custodio E (2010) Las aguas subterráneas como elemento básico de la existencia de numerosos humedales. *Ingeniería del Agua* 17:119–135

Dapeña C (2008) Isótopos ambientales livianos: su aplicación en hidrología e hidrogeología. PhD thesis. Departamento de Ciencias Geológicas, Facultad de Ciencias Exactas y Naturales, Universidad de Buenos Aires. Tesis 4282. p 442

Dapeña C, Panarello HO (1999) Development of the National Network for Isotopes in Precipitation of Argentina. II South American Symposium on Isotope Geology 503–508

Dapeña C, Panarello HO (2008) Isótopos en precipitación en Argentina. Aplicaciones en Estudios Hidrológicos e Hidrogeológicos. IX Congreso Latinoamericano de Hidrología Subterránea. ALHSUD Volumen CD T-100. p 8. Quito, Ecuador

de Montety V, Radakovitch O, Vallet-Coulomb C, Blavoux B, Hermitte D, Valles V (2008) Origin of groundwater salinity and hydrogeochemical processes in a confined coastal aquifer: case of the Rhône delta (Southern France). *Appl Geochem* 23(2008): 2337–2349

Durán JJ (2003) Presencia de aguas de diferente salinidad y origen en los humedales del litoral mediterráneo español. In: Tecnología de la intrusión de agua de mar en acuíferos costeros: países mediterráneos, 2:149–154. Serie: Hidrogeología y Aguas Subterráneas, 8, IGME. Madrid

Erskine AD (1991) The effect of tidal fluctuations on a coastal aquifer in the UK. *Ground Water* 29:556–562

Fass T, Cook PG, Stieglitz T, Herczeg AL (2007) Development of saline groundwater through transpiration of sea water. *Ground Water* 45(6):703–710

Ferris JG (1951) Cyclic fluctuations of water level as a basis for determining aquifer transmissibility: Int Geodesy Geophys Union, Assoc Sci Hydrol Gen. Assembly, Brussels, 2: 148–155; duplicated 1952 as US Geological Survey Ground Water Note 1

Fitzpatrick RW, Merry RH, Cox JW (2000) What are saline soils? What happens when they are drained? *J Aust Assoc Nat Resour Manag (AANRM)*. Special Issue (June 2000), 26–30

Fruento O, Contrera O (2013) Laboratorio de climatología Centro Nacional Patagónico—CONICET, Puerto Madryn. [http://cenpat-conicet.gov.ar/fisicambien/Rep\\_Clim\\_Mens.htm](http://cenpat-conicet.gov.ar/fisicambien/Rep_Clim_Mens.htm)

Gat JR (1981) Groundwater. In: stable isotope hydrology: deuterium and oxygen-18 in the water cycle. Technical report series No 210, International Atomic Energy Agency, Vienna, Chapter 10:223–240

Gonfiantini R (1978) Standards for stable isotope measurements in natural compounds. *Nature* 271:534

Gonfiantini R, Araguas-Araguas L (1988) Los isótopos ambientales en el estudio de la intrusión marina. Tecnología de la intrusión en acuíferos costeros, vol 1, 135–190. *Inst Geol y Minero de España, Madrid*

- Haller M, Monti A, Meinster C (2001) Hoja Geológica 4366-1 Península Valdés. Boletín Nro. 266. Buenos Aires: Servicio Geológico Minero Argentino
- Han DM, Kohfahl C, Song XF, Xiao GQ, Yang JL (2011) Geochemical and isotopic evidence for paleo-seawater intrusion into the south coast aquifer of Laizhou Bay. *China Appl Geochem* 26:863–883
- Harbison J, Cox M (2002) Hydrological characteristics of groundwater in a subtropical coastal plain with large variations in salinity, Pimpana, Queensland. *Aust Hydrol Sci J* 47(4): 651–665
- Hydrografía Naval Argentina (2010–2012) Tablas de marea. [http://www.hidro.gov.ar/oceanografia/Tmareas/Form\\_Tmareas.asp](http://www.hidro.gov.ar/oceanografia/Tmareas/Form_Tmareas.asp)
- IAEA/WMO (2002) Global network for isotopes in precipitation. The GNIP Database. <http://isohis.iaea.org>
- Lee JY, Song SH (2007) Groundwater chemistry and ionic ratios in a western coastal aquifer of Buan, Korea: implication for seawater intrusion. *Geosci J* 11(3):259–270
- Lis G, Wassenaar LI, Hendry MJ (2008) High-precision laser spectroscopy D/H and 18O/16O measurements of microliter natural water samples. *Anal Chem* 80:287–293
- Manzano M, Borja F, Montes C (2002) Metodología de tipificación hidrológica de los humedales españoles con vistas a su valoración funcional y a su gestión. Aplicación a los humedales de Doñana. *Boletín Geológico y Minero*, 113(3):313–330
- Mitsch WJ, Gosselink JG (2000) *Wetlands*, 3rd edn. Wiley, New York
- Ridd PV, Stieglitz T (2002) Dry season salinity changes in arid estuaries fringed by mangroves and saltflats. *Estuar Coast Shelf Sci* 54(6):1039–1049
- Ríos I (2010) Geoecología de plantas vasculares en suelos hidromórficos de una marisma patagónica: propiedades morfológicas, físicas, químicas y bióticas. Universidad Nacional de la Patagonia San Juan Bosco, Puerto Madryn, p 57
- Ríos I, Bouza PJ, Sain CL, Bortolus A, Cortés EG (2012) Caracterización y clasificación de los suelos de una marisma patagónica, NE del Chubut. XIX Congreso Latinoamericano de Suelos and XXIII Congreso Argentino de la Ciencia del Suelo. Mar del Plata, Argentina. Extended abstract. CD-ROM. ISBN 978-987-1829-11-8
- Schlumberger (2010) AquaChem 2010.1. A professional application for water quality analysis, plotting, replotting and modeling. Schlumberger Water Services
- Silvestri S, Marani M (2004) Salt-marsh vegetation and morphology: basic physiology, modelling and remote sensing. In: Fagherazzi S, Blum L, Marani M (eds) *Ecogeomorphology of tidal marshes*. American Geophysical Union, Coastal and Estuarine Monograph Series Observations, Washington
- Smith AJ, Hick WP (2001) Hydrogeology and aquifer tidal propagation in Cockburn sound, Western Australia. CSIRO Technical report 6/01
- Soil Survey Staff (1999) Soil taxonomy. A basic system of soil classification for making and interpreting soil surveys; second edition. *Agricultural Handbook 436*; Natural Resources Conservation Service, USDA, p 869, Washington
- Thornthwaite CW, Mather JR (1957) Instructions and tables for computing potential evapotranspiration and water balance. Centerton, p 312
- Vázquez Suñé E (2002) Programa Easy Quim 4. GHS-UPC, CIHS, Spain
- Vengosh A (2003) Salinization and saline environments. In: Sherwood Lollar B, Holland HD, Turekian KT (eds) *Environ Geochem*. Elsevier Science. 9:333–365
- Warner N, Lgourna Z, Bouchaou L, Boutaleb S, Tagma T, Hsaissoune M, Vengosh A (2013) Integration of geochemical and isotopic tracers for elucidating water sources and salinization of shallow aquifers in the sub-Saharan Drâa Basin, Morocco. *Appl Geochem* 34:140–151
- Wilson AM, Morris JT (2012) The influence of tidal forcing on groundwater flow and nutrient exchange in a salt marsh-dominated estuary. *Biogeochemistry* 108(1–3):27–38. doi:10.1007/s10533-010-9570-y
- Yurtsever Y (1994) Role of environmental isotopes in studies related to salinization processes and salt water intrusion dynamics. In: *Proceedings of the 13th Salt-Water Intrusion Meeting*, Cagliari. pp 177–185